University of Iceland
Faculty of Natural Sciences
Department of Physics

Coulomb and Spin-Orbit Interaction Effects in a Mesoscopic Ring

by

Csaba Daday

A thesis submitted in partial satisfaction
of the requirements for the degree of Master of
Science in Physics at the University of Iceland

Committee in charge:
Viðar Guðmundsson, Chair
Andrei Manolescu

Reykjavík
August 2011

Abstract

We study a ring structure on a two-dimensional electron gas with both Rashba and Dresselhaus spin-orbit interaction in an external magnetic field. The competition between the two kinds of SOI leads to a deformation of the charge and spin densities around the ring. After examining the one-electron eigenstates we investigate Coulomb effects. We use two different ring models: a continuous model with analytical single particle states (Tan-Inkson) and a discrete model (tight-binding) which is more convenient for many-body calculations. We show that for more than two electrons the deformation of the charge density is smeared out by the Coulomb interaction, whilst the deformation of the spin density is amplified.

Contents

List of Tables

List of Figures

Acknoledgements

I would like to thank first of all my supervisor, Andrei Manolescu who helped me throughout these two years, teaching me much about Physics, but also assisting me in dealing with paperwork and other problems in Iceland. It was a privilige to work together with him, and I learned much from discussions with him. His wife, Ileana, has been a great host every time I visited them, and a source of interesting and entertaining conversations.

I am indebted to Viðar Guðmundsson, who has taught me many new ideas in Physics and also helped me through many administrative issues in the University. I am also thankful for the help I got from Cătălina Marinescu in writing this thesis. She came with a fresh perspective which I feel improved the thesis substantially.

I would like to thank Anton, Gunnar and Kristinn for helping me with all sorts of technical problems and help with the Icelandic language.

I am also very grateful to my teachers from Romania, Károly Bogdán and István Bartos-Elekes from high school and the Physics professors from Cluj, in particular Mircea Crişan, my undergraduate supervisor and Titus Beu for introducing Quantum Mechanics to me.

My family has supported me through these two years as warmly and closely as they had through my entire life, despite the great physical distance between Iceland and Romania. I fondly remember my grandfather, Zsolt Sr, who was perhaps the first to inspire me to study the exact sciences through his logical riddles. Sadly he passed away before he could see how deeply he affected me.

I would like to mention the proofreading and patient advice regarding my thesis that I got from Sietske, Helene and Mateusz. Thank you!

This thesis is the output of a research project supported by the Icelandic Research Fund under the Grant for Excellence 090025011/2009 (Computational Design of Materials and Devices, or Reknisetur fyrir hönnunefna og íhluta), which is a large joint research program of University of Iceland and Reykjavik University. The research was carried out at Reykjavik University under the supervision of Prof. Andrei Manolescu

and co-supervised by Prof. Viðar Guðmundsson from University of Iceland.

Notation

Unless otherwise stated, the following conventions shall be followed throughout this paper:

SOI spin-orbit interaction

θ angular coordinate

r radial coordinate

ρ adimensional radius

φ wavefunctions corresponding to basis (pure) states

ψ one-electron eigenfunctions

m quantum number corresponding to angular momentum

m^* electron effective mass

m_0 free electron mass

α Rashba SOI constant

β Dresselhaus SOI constant

χ Radial wavefunctions

∂_{q_i} short form of $\frac{\partial}{\partial q_i}$

$\leftarrow$ assignment operator

K Coulomb constant of material, as in $V(r) = Ke^2/r$

Chapter 1

Introduction

1.1 Spintronics

Spintronics seeks to create devices where the spin degree of freedom is used alongside, or instead of, charge currents. These devices could have a large variety of applications, including information encoding, transmission, processing, etc. It is predicted that such devices would have lower power consumption, shorter switching times and more stable states [2, 3]. A stable system that is a superposition of two orthogonal states is essential to quantum computing: therefore spintronic devices are hoped to become efficient implementations of qubits.

The first such proposal was made by Datta and Das in 1990 [4]. They introduced the concept of using spin in processing information, proposing an 'Electric analog of the electro-optic modulator'. This device would polarize an electron beam much like electro-optic modulators polarize a photon beam (ray of light). Today such a device is known as a Spin-Field Effect Transistor and its experimental realization at room temperature was groundbreaking news recently [5], about 20 years after the Datta and Das paper.

There are two main ways of creating and changing spin polarisation: via magnetic fields of AC currents, i.e. Zeeman interaction [6], or via electric fields and spin-orbit interaction. In general, electric manipulation of spin polarization is to be preferred to magnetic manipulation for various reasons (e.g. compatibility with existing electronic devices) [2]. In modern literature spin-orbit coupling is considered more important than the Zeeman effect in spintronics. We will now proceed to give a short description of SOI.

1.2 Spin-orbit interaction

In the single particle Hamiltonian, SOI is represented by a term proportional with spin and momentum. It is caused by an electric field and the magnetic component of its Lorentz transform. Its simplest case is the so-called Pauli SOI for core electrons: in this case the electric field close to the nucleus is strong enough so that its effects are significant even at non-relativistic momenta. The strength of the Pauli SOI is referred to as spin-orbit splitting Δ_{SO}. In some semiconductors the spin-orbit splitting gap is of similar amplitude to the band gap. In these materials the strength of spin-orbit coupling is enhanced and will have significant effects also in the conduction band.

Rashba first introduced the SO coupling named today after him in 1955 [7]. This kind of SOI is caused by the structure inversion assymetry of a 2DEG system. It has the following Hamiltonian: $H_R = \frac{\alpha}{\hbar}(\sigma_x p_y - \sigma_y p_x)$ The coupling strength α is directly tunable by an external electric field created by gates or electrodes. Table 1.2 [1] reveals clearly that the Rashba constant strongly depends on the experimental set-up.

Dresselhaus introduced another kind of SO coupling which exists in zinc blende structures and is caused by structure inversion assymetry [8]. The zinc blende structure is geometrical identical to the diamond structure, but because alternative atoms are different (as opposed to the diamond structure), the inversion symmetry is broken. In the original paper the interaction was deduced via group theoretical arguments, but a more modern approach is to use the $\mathbf{k} \cdot \mathbf{p}$ method, as described by e.g. [9]. Table 1.1 [1] gives some values of β. Note that in the cases with the highest coupling constants the band gap E_g is comparable to, or even smaller than, the SO splitting Δ_{SO}. The Dresselhaus SOI in a 2D system has the following Hamiltonian: $H_D = \frac{\beta}{\hbar}(\sigma_x p_x - \sigma_y p_y)$ The coupling strength in a 2D case has the formula $\beta = \left(\frac{\pi}{d}\right)^2 \beta_{3D}$ where β_{3D} is the bulk Dresselhaus constant and d is the thickness. The thickness is important because it determines the normal momentum k_z as per the uncertainty principle.

1.3 Quantum rings and spin-orbit coupling

Quantum rings have often been suggested as spintronic devices, particularly as potential implementations of qubits. Compared to quantum dots they promise less spin relaxation and thus more stable quantum bits [10].

Spin-orbit coupling in a ring structure has been extensively studied in recent years [11–16].

Ref [17] established the correct 1D Hamiltonian for Rashba SOI, different from some earlier literature. They noted that earlier works had clearly erred since the emerging Hamiltonian was non-Hermitian.

Table 1.1: SO splitting, band gap, effective mass and Dresselhaus SOI strength of various semiconductors [1]

Material	Δ_{SO} (eV)	E_g (eV)	$m^*(m_0)$	β_{3D} (meV Å^3)
AlAs	0.28	3.1	0.15	11.55
AlP	0.07	3.63	0.22	2.11
AlSb	0.67	2.39	0.14	41.50
GaAs	0.34	1.51	0.067	24.45
GaP	0.08	2.88	0.13	-2.42
GaSb	0.76	0.81	0.039	178.51
InAs	0.38	0.41	0.026	48.63
InP	0.11	1.42	0.08	-10.34
InSb	0.81	0.24	0.014	473.61

Table 1.2: Rashba SOI strength of various 2DEG setups [1]

Material	α (meV Å)
AlSb/InAs/AlSb	60
AlSb/InAs/AlSb	0
AlSb/InAs/AlSb	0
AlGaSb/InAs/AlSb	$120 - 280$
InAlAs/InGaAs/InAlAs	40
InAlAs/InGaAs/InAlAs	$63 - 93$
InAlAs/InGaAs/InAlAs	$50 - 100$
InGaAs/InAs/InAlAs	$60 - 110$
InGaAs/InAs/InAlAs	$200 - 400$
InGaAs/InP/InGaAs	$63 - 153$
Si/SiGe QW	$0.03 - 0.12$
SiO_2/InAs	$100 - 300$

Refs [12] and [16] use 1D rings with non-interacting electrons and Rashba interaction and continued to investigate transport properties. Note that this is the only case where analytical solutions are still retained. 2D rings, or 1D rings with both kinds of SOI together can only be solved numerically. Ref [14] also uses the Dresselhaus interaction, in both 1D and 2D systems; they note that the in the case of both Rashba and Dresselhaus SOI, an effective periodic potential exists that breaks angular symmetry and that creates localization. Refs [11] and [13] both introduce Coulomb interaction in this picture; however, they only deal with exactly two electrons.

Original research

Our research aims to go slightly further: to include Coulomb interaction with more than two electrons. Our method, exact diagonalization, makes it possible to treat a larger number of electrons, and the limit to this number is only determined by computational time. We will have $N = 2, 3,$ or 4 in this paper. We have had some trials with the discrete model with N as high as 6.

The basic system will be a InAs ring with radius of $r = 100$nm. We used standard values for material parameters: Landé g-factor $g^* = -14.9$, effective mass $m^* = 0.023m_0$ and SOI strengths $\alpha = 50$ meVnm, $\beta = 30$ meVnm.

The one-electron Hamiltonian of our system looks like:

$$H(r) = H_O + H_{SO} + H_Z + V(\mathbf{r}) \tag{1.1}$$

H_O being the orbital (cinetic) term, H_{SO} is the spin-orbit interaction, H_Z is the Zeeman term and $V(\mathbf{r})$ is a scalar potential. The magnetic field is included in the orbital term. In the case of the continuous model, there are analytical eigenstates for H_O.

Outline

The remainder of this article is organized as follows. Section 2 will describe the discrete model and results obtained by it. Section 3 describes the Tan-Inskon basis and its results. Section 4 will summarize our findings. Various mathematical details will be given in the appendix.

The original results have been published in arXiv:1106.3697v1 and in the proceedings of the workshop OptoTrans2011, held in February 2011 in Berlin, at the Weierstrass Institute for Applied Analysis and Stochastics (WIAS).

Chapter 2

Discrete model

2.1 Model description

The discrete model contains a certain number of sites situated on a number of concentric circles. Each basis state is a discrete delta function[1] centered on a particular site. This is usually referred to as the basis of position eigenvectors.

2.1.1 Scaling

Before the presentation of our results, it is important to talk about units of various quantities. If we assume $m^* = 0.023m_0$, $R_{ext} = 100$ nm we get $t_R = 0.1657$ meV and $\alpha_0 = 16.57$ meVnm. The magnetic field unit is $B_0 = 32.9$ mT. Throughout this thesis, the adimensional magnetic field has the notation $b = \frac{B}{B_0}$.

[1] a function that has value 1 at that site and 0 everywhere else.

Table 2.1: units of physical quantities

Physical quantity	unit	note
length	R_{ext}	radius
energy	$\frac{\hbar^2}{2m^* R_{ext}^2}$	natural energy unit $t_{R_{ext}}$
SOI constant	$\frac{\hbar^2}{2m^* R_{ext}}$	$t_{R_{ext}} \cdot R_{ext}$
magnetic field	$\frac{m^* t_{R_{ext}}}{\hbar e}$	cyclotron energy

2.2 One-electron states

2.2.1 One dimensional case

Making the model one-dimensional comes naturally. We took 1 circle made up of 300 sites. Fig 2.1 shows the energy spectrum vs magnetic field for a system without any Coulomb or SOI effects. However, the Zeeman effect is included. As it is clearly visible, the spectrum is made up of intertwining parabolas, as expected.

The form of the SO Hamiltonian in the 1D case is not trivial to deduce from the equations in A.3. [17] pointed out that earlier papers used a simple method (simply neglecting all terms depending of ∂_r) to get a Hamiltonian but one that turned out to be non-Hermitian. Meijer et al deduced the proper Hamiltonian using a rigorous approach: they assumed a Gaussian ring potential and at the end of their calculations it was taken to be infinitely steep. Their approach focused on the Rashba SOI but it is thereafter trivial to include the Dresselhaus term as well. This was done, for example, in Ref [14], using the units from table 2.1.1:

$$H = \left[-i\frac{\partial}{\partial\theta} + b + \frac{\overline{\alpha}}{2}\sigma_r - \frac{\overline{\beta}}{2}\sigma_\theta^*\right]^2 - \frac{\overline{\alpha}^2 + \overline{\beta}^2}{4} + \frac{\overline{\alpha}\overline{\beta}}{2}\sin 2\theta + \frac{1}{2}gb\sigma_z \qquad (2.1)$$

Fig 2.2 shows the energy spectrum of the system with only one type of SOI present. The energies are slightly lower than the ones without SOI. This is an effect that is generally true in all systems with SOI. There is no obvious difference between the Rashba and Dresselhaus interactions. In fact, it is an analytical result that the energy spectrum for (α, β, g^*) is the same as a system with $(\beta, \alpha, -g^*)$ [14]. There is a certain phase difference between the parabolas. However, if we look at the spin polarization projected on the x-y plane, there is a very clear difference. Fig 2.3 shows the spin polarization of the ground state in each case. In the case of Rashba SOI, the spin is simply radially oriented. In the case of Dresselhaus SOI, there is a more complicated orientation. It is observable that in the case of Rashba interaction, there is a spin precession that has the same angular velocity to the motion of the electron, while in the case of Dresselhaus interaction, the spin precession still has the same angular velocity, but it is in the opposite direction. This is not surprising, and it has been discussed in works such as [1, 9].

The spin polarization of the ring is also affected by spin-orbit coupling. Without SOI, states change abruptly in s_z. If SOI is present, changes in spin polarization occur more softly, because the Hamiltonian now is not diagonal in spin. This difference is illustrated in Fig 2.6. If there is no SOI then at a sufficiently large magnetic field all of the first four states are aligned with the magnetic field due to the Zeeman effect, but the SOI makes this transition more complicated.

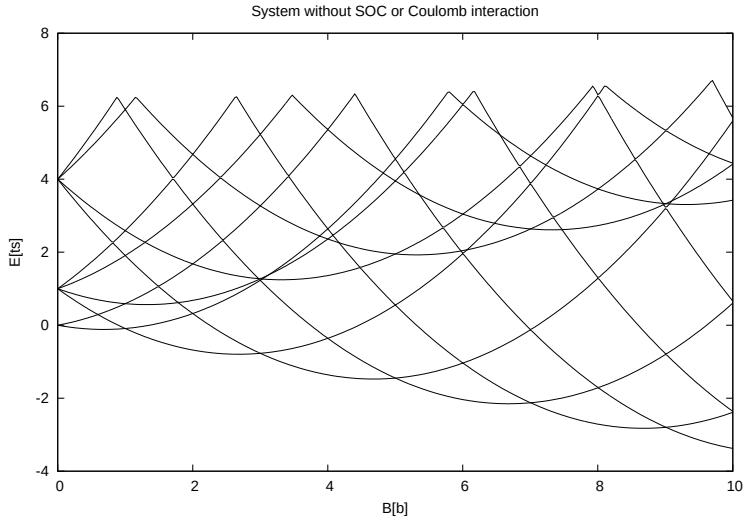

Figure 2.1: Energy spectrum for unperturbed 1D system

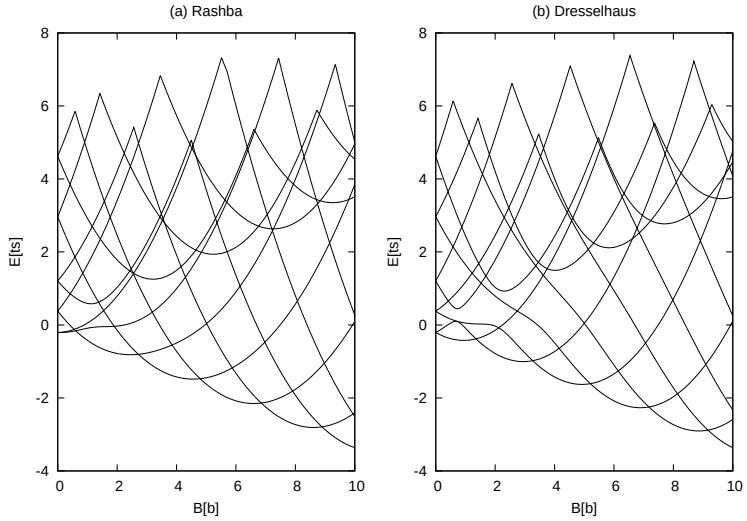

Figure 2.2: Energy spectrum for 1D system when only one type of SOI is present

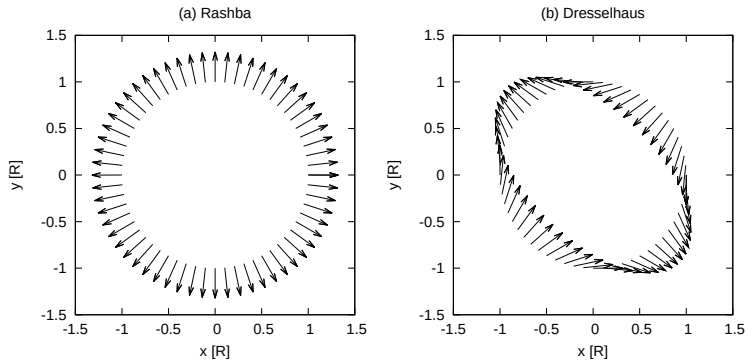

Figure 2.3: Spin orientations projected on the x-y plane along the ring in the case of each SOI

There are two interesting effects in the case when both forms of SOI are present. Fig 2.7 shows charge density along the ring. There are two clear maxima of it: at $\frac{\pi}{4}$ and $\frac{5\pi}{4}$. It is worth noting that these two maxima occur at the positions where the eigenspinors of the two individual cases are parallel (viz Fig 2.3). The other effect manifests itself in the energy spectrum. (Fig. 2.4).

In the case of both kinds of SOI, the Hamiltonian conserves a special kind of *parity* [13]. This parity of a quantum state in this case is defined as follows:

$$p(\psi) = \begin{cases} \text{odd, if} & \sigma\psi(-\mathbf{r}) = \psi(\mathbf{r}) \quad \forall \mathbf{r}, \sigma \\ \text{even, if} & \sigma\psi(-\mathbf{r}) = -\psi(\mathbf{r}) \quad \forall \mathbf{r}, \sigma \\ \text{undefined} & \text{otherwise} \end{cases} \tag{2.2}$$

The above property did indeed hold for our numerical results. Moreover, Nowak and Szafran [13] observed that states with like parity repel each other in this B-dependent spectrum. They refer to [15] but they do not point out clearly how avoided crossings in the dispersion graphs $E(k)$ relate to, or lead to those in the energy spectrum $E(B)$.

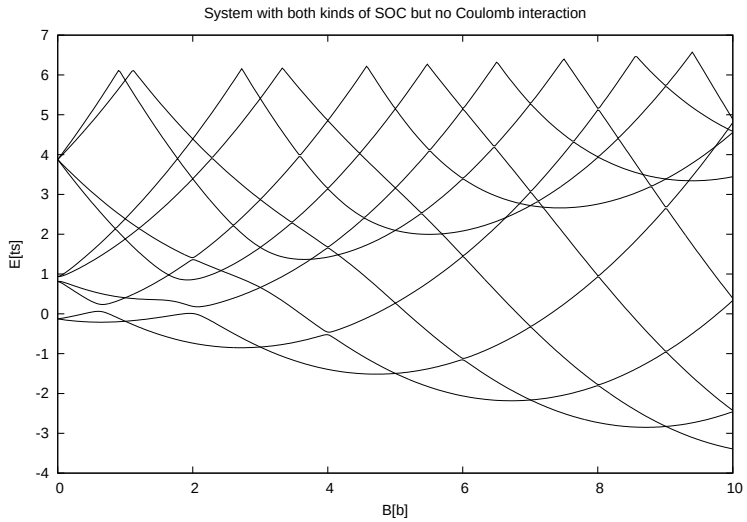

Figure 2.4: Energy spectrum for 1D system when both types of SOI are present

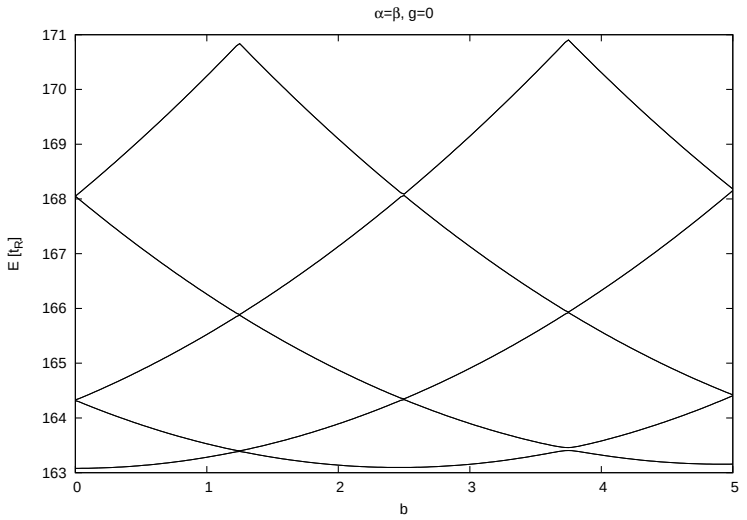

Figure 2.5: Energy spectrum for a 2D ring in the special case $\alpha = \beta, g = 0$. Note that each energy is doubly degenerate.

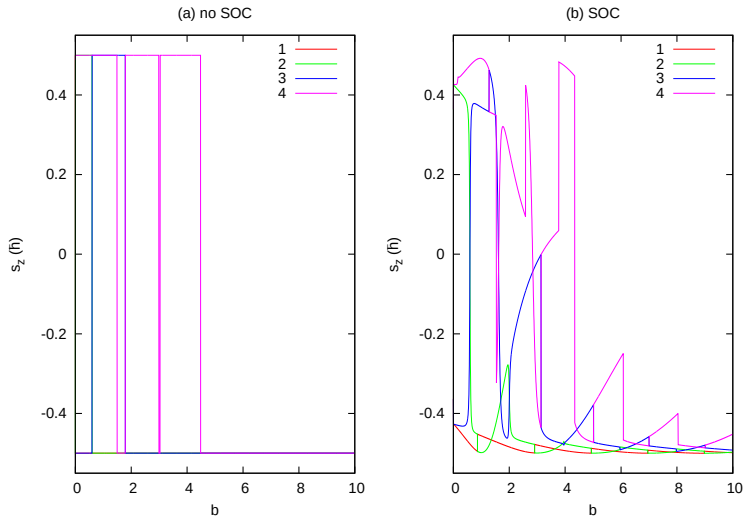

Figure 2.6: Spin polarization along the z axis

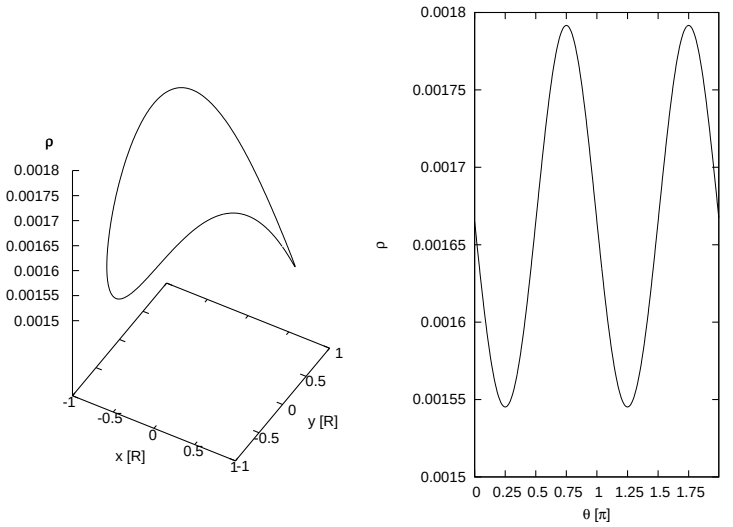

Figure 2.7: Charge density along the ring and as a function of angle

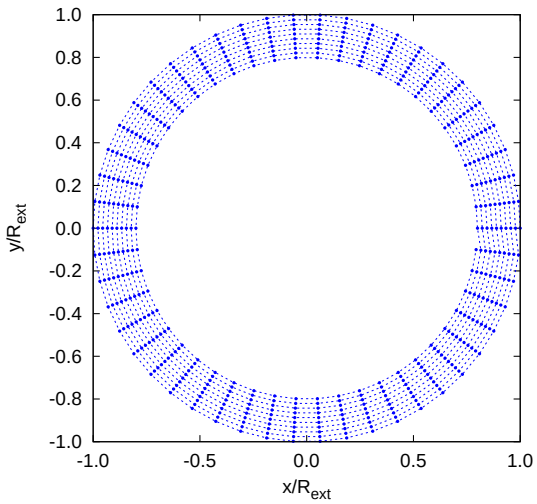

Figure 2.8: Position of sites in the 2D case

2.2.2 Two dimensional case

The sample consists of 10 concentric circles with the ratio between radii $R_{int} = 0.8R_{ext}$ with 50 sites each. Fig 2.8 shows their alignment.

The energy spectrum and spin polarization will be similar to the 1D case. However, in the 2D case there is a net diamagnetic effect, i.e. a parabolic rise in energy. At very large magnetic fields electrons would have a rotation with a very small radius because of the strong Lorentz force, this rotation would be nearly independent of the actual ring radius. It is clear that the discrete ring model is not suitable for this domain, since there are insufficient sites to cater to such motion. This is one area where the continuous model is superior to the discrete.

In Nowak and Szafran's paper they observed that in the special case $\alpha = \beta$; $g = 0$ the gaps caused by avoided crossings close as every state is parity-degenarate. Again, their reasoning seems inadequate to prove that the self-avoiding disappears altogether. Nevertheless, in the discrete case we have successfully confirmed this to a certain degree. Fig 2.5 shows how the gaps almost completely close. There is always a slight error due to the diamagnetic effect so it seems reasonable to conclude that they would indeed close with perfect calculations. However, this prediction is not particularly important seeing as there is no practical way of setting $g = 0$, as opposed to α and β,

which both may be tuned on a reasonably wide range.

2.3 Interacting states

2.3.1 Exact diagonalization

The many-body Hamiltonian of a system of electrons is, in general:

$$H = \sum_{i}^{N_e} \frac{p_i^2}{2m_0} + \frac{1}{2} \sum_{i \neq j}^{N_e} \frac{Ke^2}{|\mathbf{r_i} - \mathbf{r_i}|} \tag{2.3}$$

To solve this equation (or the one which includes the SOI), we need a many-body basis. The complete procedure consists of first calculating some one-electron eigenstates (which we have done in the previous section) and then taking the first N_s states. We then assume that electrons can occupy only one of these first states. The many-body basis states are then bitstrings of N_s bits, out of which exactly N_e are ones. The many-body matrix will have a dimension of $N_{mb} = \binom{N_s}{N_e}$. N_e is the number of electrons in our system, which in our calculations is a well-defined number. N_s should be a number that is at least a few times larger than N_e. The minimum N_s for which our results are reliable needs to be determined empirically. In our case, we used $N_e = 2 : N_s = 8, N_{mb} = 56$; $N_e = 3 : N_s = 10, N_{mb} = 120$ $N_e = 4 : N_s = 12, N_{mb} = 495$.

$$\{\mu\} = \left\{ \mid i_1^\mu, i_2^\mu, \ldots, i_{N_s}^\mu \right\rangle, \sum i^\mu = N_e \right\} \tag{2.4}$$

The matrix elements of the many-body Hamiltonian are (μ and ν being indexes of bitstrings):

$$\langle \mu \mid H \mid \nu \rangle = \sum_a E_a i_a^\nu \delta_{\mu\nu} + \frac{1}{2} \sum_{a,b,c,d} V_{abcd} \left\langle \mu \mid c_a^+ c_b^+ c_d c_c \mid \nu \right\rangle \tag{2.5}$$

c are fermionic annihilation operators and c^+ creation operators. I will proceed to give a short description of how they act on these bitstrings, based largely on [18]. Let us consider a many-body state $|\mu\rangle = |i_1^\mu, i_2^\mu, \ldots\rangle$ and an annihilation operator c_a. Then

$$c_a |\mu\rangle = \begin{cases} (-1)^{s_a} \left| \ldots, i_{a-1}^\mu, 0, i_{a+1}^\mu, \ldots \right\rangle & i_a^\mu = 1 \\ 0 & i_a^\mu = 0 \end{cases} \tag{2.6}$$

$$c_a^+ |\mu\rangle = \begin{cases} 0 & i_a^\mu = 1 \\ (-1)^{s_a} \left| \ldots, i_{a-1}^\mu, 1, i_{a+1}^\mu, \ldots \right\rangle & i_a^\mu = 0 \end{cases} \tag{2.7}$$

Here $s_a = \sum_j^{j<a} i_j^\mu$, i.e. a number that shows the number of occupied states that are lower than a. From these we can conclude that

$$c_a c_b \left|\mu\right\rangle = \begin{cases} (-1)^{s_a^\mu + s_b^\mu} \left|\mu(i_a^\mu \leftarrow 0, i_b^\mu \leftarrow 0)\right\rangle & i_a^\mu = i_b^\mu = 1, a < b \\ (-1)^{s_a^\mu + s_b^\mu - 1} \left|\mu(i_a^\mu \leftarrow 0, i_b^\mu \leftarrow 0)\right\rangle & i_a^\mu = i_b^\mu = 1, a > b \\ 0 & \text{otherwise} \end{cases} \tag{2.8}$$

Note that $c_b c_a \left|\mu\right\rangle = -c_a c_b \left|\mu\right\rangle$

The elements V_{abcd} are Coulomb terms, obtained in general as:

$$V_{abcd} = \int \psi_a^*(\mathbf{r}) \psi_b^*(\mathbf{r}') \frac{Ke^2}{|\mathbf{r} - \mathbf{r}'|} \psi_c(\mathbf{r}) \psi_d(\mathbf{r}')\, d\mathbf{r}\, d\mathbf{r}' \tag{2.9}$$

Bearing in mind that $\psi_a(\mathbf{r}) = \sum_i c_{ia} \varphi_i(\mathbf{r})$, $\forall a$ we can rewrite the above equation into:

$$V_{abcd} = \sum_{i,j,k,l} c_{ia}^* c_{jb}^* c_{kc} c_{ld} U_{ijkl} \tag{2.10}$$

where

$$U_{ijkl} = \int \varphi_i^*(\mathbf{r}) \varphi_j^*(\mathbf{r}') \frac{Ke^2}{|\mathbf{r} - \mathbf{r}'|} \varphi_k(\mathbf{r}) \varphi_l(\mathbf{r}')\, d\mathbf{r}\, d\mathbf{r}' \tag{2.11}$$

In the discrete case the above integral will be transformed into a sum:

$$U_{ijkl} = \sum_{n_1=1}^{N_{sites}} \sum_{n_2=1}^{N_{sites}} \delta_{i,n_1} \delta_{j,n_2} \delta_{ik} \delta_{jl} \frac{Ke^2}{|\mathbf{r}_{n_1} - \mathbf{r}_{n_2}|} \tag{2.12}$$

The question of singular terms in the sum is a valid one, but it turns out that in the continuous limit they go to zero.

The terms $\left\langle \mu \mid c_a^+ c_b^+ c_d c_c \mid \nu \right\rangle$ depend only on the bit-strings and can be expressed as a scalar product:

$$\left\langle \mu \mid c_a^+ c_b^+ = (\, c_b c_a \mid \mu \rangle)^\dagger \tag{2.13}$$

$$\left\langle \mu \mid c_a^+ c_b^+ c_d c_c \mid \nu \right\rangle = \left\langle \mu_{ba} \mid \nu_{dc} \right\rangle \tag{2.14}$$

where $\left|\mu_{ab}\right\rangle = c_a c_b \left|\mu\right\rangle$. Keeping in mind that our basis states are orthonormal in the many-body space, we can write that

$$\left\langle \mu_{ba} \mid \nu_{dc} \right\rangle = \begin{cases} -1 \\ 1 \\ 0 \end{cases} \tag{2.15}$$

It will be 0 whenever the bits are not completely identical and its sign will depend on the order of the annihilation operators c_a, c_b, c_c, c_d.

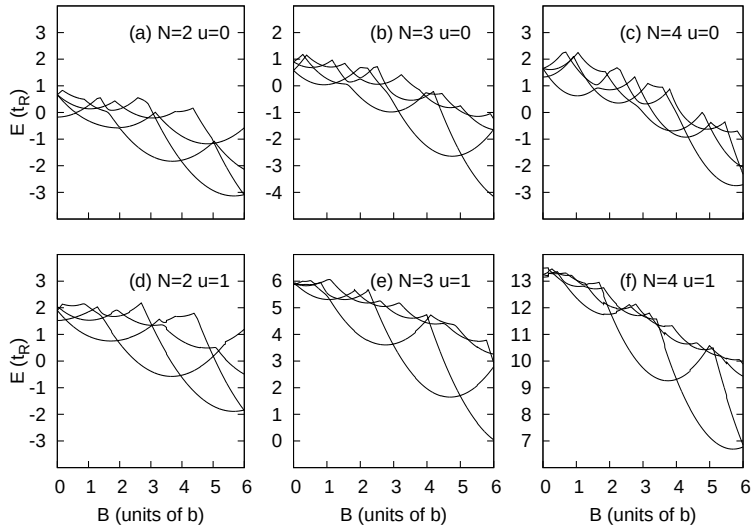

Figure 2.9: Energy spectra for 1D case: 2, 3, and 4 electrons, with/without interaction.

2.3.2 Results

In both 1D and 2D cases, the Coulomb interaction does not alter the energy spectrum in a major way. Fig 2.9 and Fig 2.10 show the spectra for $2, 3,$ and 4 electrons.

To study the charge density deformation quantitatively, we calculated the standard deviation of charge density along the sites on the 6-th circle and see how this standard deviation behaves as the magnetic field changes. The standard deviation behaves slightly surprisingly when there are exactly two electrons and the Coulomb interaction is present. The standard deviation increases significantly. For $N = 3, 4$ the charge density deviation all but disappears. In the 1D case the deviation decreases even for $N = 2$.

The physical explanation for the increased density deviation is not obscure. Assuming an electron is localized somewhere on a circle, it creates a potential that has a minimum on the diametrically opposed point. The Coulomb repulsion for the case $N = 2$ only makes the valley of the SOI effective potential steeper because the two potentials both determine valleys at diametrically opposed points.

The net spin polarization along the z axis also changes on account of the Coulomb interaction. Fig 2.12 compares the cases with and without interaction. It is interesting to see that the Coulomb interaction enhances the Zeeman effect, i.e. spin polarization

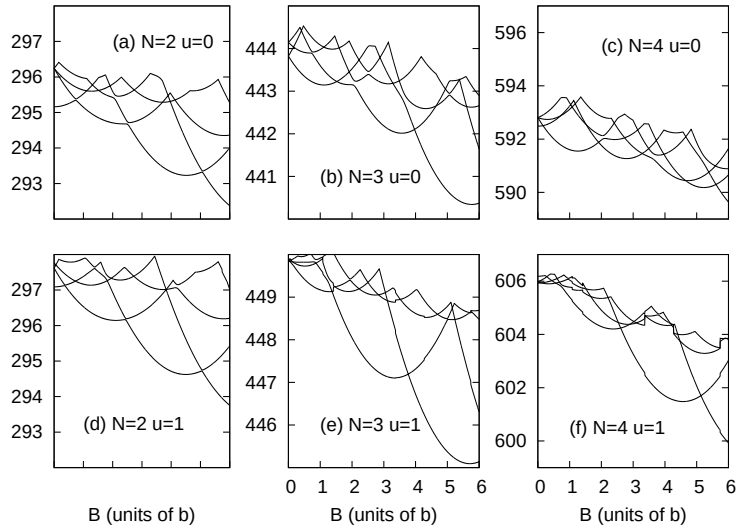

Figure 2.10: Energy spectra for 2D case: 2, 3, and 4 electrons, with/without interaction

reaches saturation at a smaller magnetic field, especially for the ground state. Fig 2.13 analyzes the standard deviation of spin polarization. This time it is clear that the Coulomb interaction increases the amplitude of spin deviation.

Collective states

There is an interesting phenomenon that occurs only in the presence of the Coulomb interaction. If the ring is placed in a uniform electric field and SOI and Coulomb interaction are both present, there are some unusually large charge deformations in a few excited states. They might be associated with collective modes also known as plasma oscillations or plasmons. The electric field is weak and it does not produce any significant changes in the charge density by itself. These excited states could be named 'collective' because they only occur when there is interaction between the electrons. We have done extensive analysis of these states, but more investigation is needed to make any quantitative conclusions about this phenomenon.

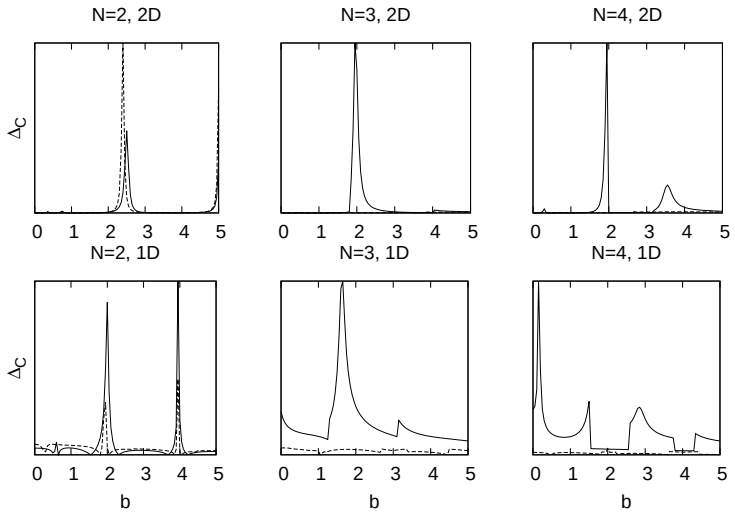

Figure 2.11: Standard deviation of charge density without (solid) and with (dashed) interaction

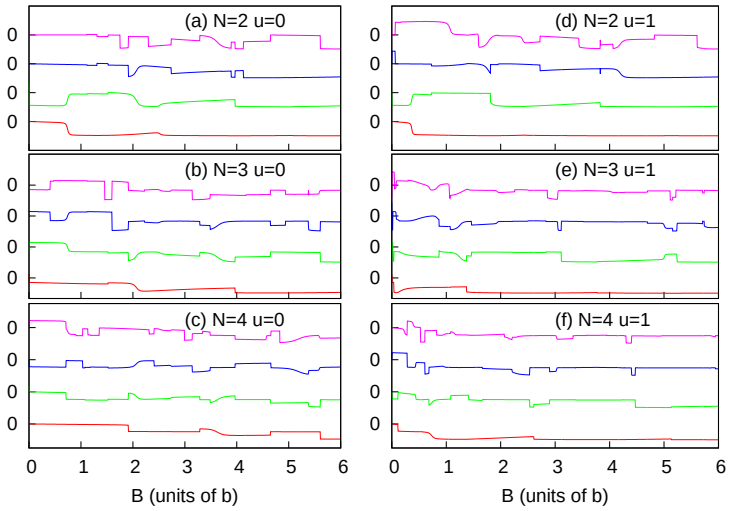

Figure 2.12: Net spin polarization along the z-axis for 2, 3 and 4 electrons, with/without interaction Note the scale is $s_z = -\frac{N\hbar}{2}.. + \frac{N\hbar}{2}$, where $N = 2, 3, 4$ is the number of electrons

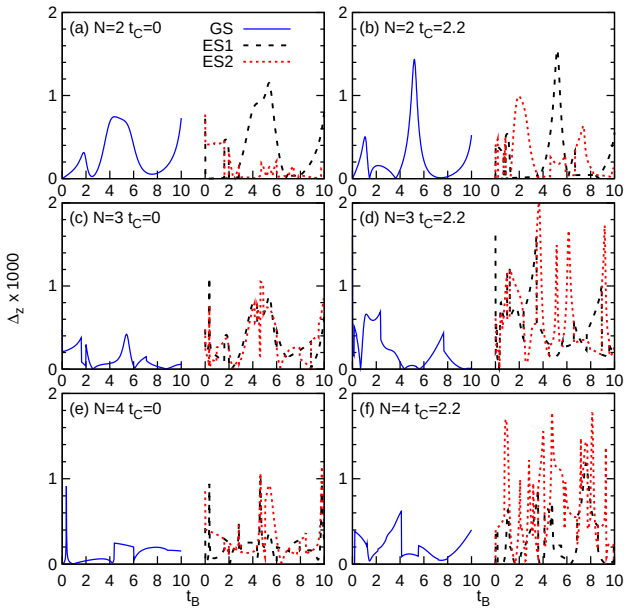

Figure 2.13: Standard deviation of spin polarization for the ground state (left) and the first two excited states (right)

Chapter 3

Continuous model

3.1 Model description

Tan and Inkson proposed [19] a new ring potential. Its basic form is given by:

$$V(r) = \frac{a_1}{r^2} + a_2 r^2 - 2\sqrt{a_1 a_2} \tag{3.1}$$

. This potential has a minimum $V = 0$ at r_0:

$$r_0 = \sqrt[4]{\frac{a_1}{a_2}} \tag{3.2}$$

. Fig. 3.1 shows the form of the Tan-Inkson potential for a few sets of parameters a_1, a_2. In the first and fourth cases $r_0 = 100$ nm, in the second case $r_0 = 90$ nm and in the third case $r_0 = 110$ nm.

Close to this minimum the potential has a parabolic behavior:

$$V(r) \approx \frac{1}{2} m^* \omega_0^2 (r - r_0)^2, \tag{3.3}$$

where the angular frequency ω_0 is given by:

$$\omega_0 = \sqrt{\frac{8a_2}{m^*}}. \tag{3.4}$$

It is more convenient to describe the Tan-Inkson potential using the mean radius r_0 and

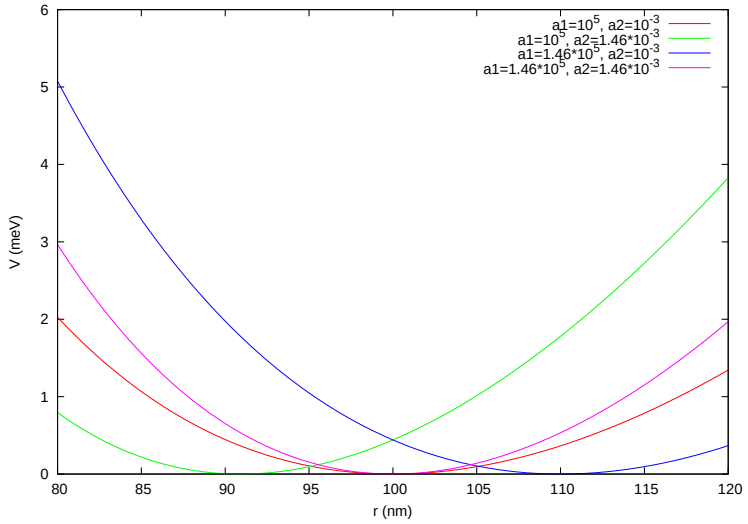

Figure 3.1: Tan-Inkson potential for four different sets of values of a_1, a_2

the confinement potential V_{conf}, given by:

$$r_0 = \sqrt[4]{\frac{a_1}{a_2}}, \quad V_{conf} = \hbar\omega_0 = \hbar\sqrt{\frac{8a_2}{m^*}} \tag{3.5}$$

They proved that such a potential would give analytical solutions of the Schrödinger equation. The exact deduction is given in the Appendix.

$$\varphi_{nm}(\rho,\theta) = A_{nm} e^{im\theta} \rho^M e^{-\frac{\rho^2}{4}} L_n^M(-\frac{\rho^2}{2}) \tag{3.6}$$

where

$$\rho = \frac{r}{\lambda}, \quad M = \sqrt{m^2 + \left(\frac{m^*}{2\hbar}\omega_0 r_0^2\right)^2} \tag{3.7}$$

λ is the effective magnetic length, given by:

$$\lambda = \sqrt{\hbar m^*} \cdot \sqrt{\frac{1}{e^2B^2 + \omega_0^2 m^{*2}}} \tag{3.8}$$

The normalization constant A_{nm} is:

$$A_{nm} = \frac{1}{\lambda^{M+1}} \sqrt{\frac{n!}{\pi 2^{M+1} \Gamma(M+n+1)}} \tag{3.9}$$

The quantum number $n = 0, 1, 2, \ldots$ shows the order of the radial mode and $m = 0, \pm 1, \pm 2, \ldots$ gives the angular momentum. The energy spectrum will look like this:

$$E_{n,m} = \left(n + \frac{1}{2} \left(\sqrt{m^2 + \left(\frac{m^*}{2\hbar} \omega_0 r_0^2 \right)^2} + 1 \right) \right) \hbar\omega - \frac{m}{2} \hbar\omega_c - \frac{m^*}{4} \omega_0^2 r_0^2 \tag{3.10}$$

Two other frequencies that appeared above: $\omega_c = \frac{eB}{m^*}$ is the cyclotron frequency and $\omega = \sqrt{\omega_0^2 \omega_c^2}$ is the effective cyclotron frequency. The dependence of $E_{n,m}$ of n is a simple linear one, but that of m is not straightforward, see eq. 3.10.

For zero magnetic field and $m \ll \frac{m^*}{2\hbar} \omega_0 r_0^2$, the dependence is simply parabolic, but for a larger magnetic field, it has a more complicated form and it is no longer centered around $m = 0$. Fig 3.2 shows this, with the following parameters: $E_{conf} = 10\text{meV},\ r_0 = 100$ nm and for $n = 0$.

The physical explanation is that states with a positive angular momentum ($m > 0$) are slowed down by the magnetic field.

It is also instructive to look at the B-dependence of the energy spectrum (Fig 3.3). They are intertwined parabolas. Each parabola represents one particular angular momentum. As the magnetic field increases, the lowest states will have larger angular momentum. The spectrum is a physical observable and it is not a particular characteristic of the Tan-Inkson model. For example, it looks qualitatively identical to the discrete case.

3.2 One-electron states

3.2.1 Spin-orbit interaction

The Hamiltonian for both Rashba and Dresselhaus SOI:

$$H_{SO} = \frac{\alpha}{\hbar}(p_y \sigma_x - p_x \sigma_y) + \frac{\beta}{\hbar}(p_x \sigma_x - p_y \sigma_y) \tag{3.11}$$

where

$$\begin{aligned} p_x &= -i\hbar \frac{\partial}{\partial x} + eA_x \\ p_y &= -i\hbar \frac{\partial}{\partial y} + eA_y \end{aligned}$$

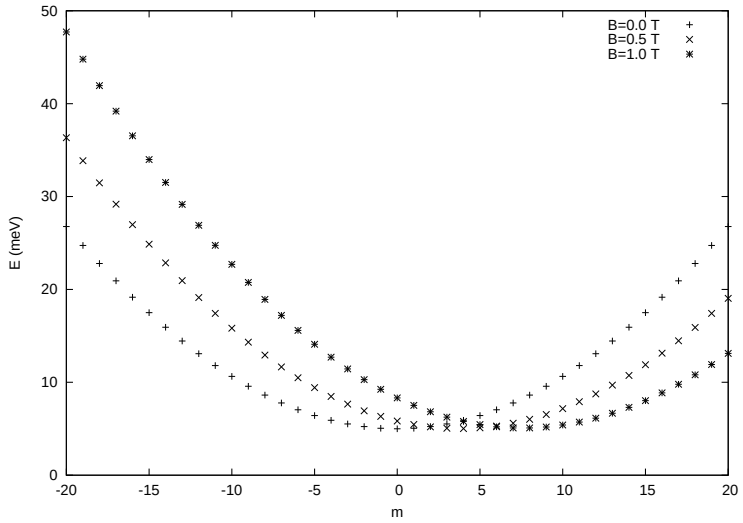

Figure 3.2: Dependence of single-electron energy on quantum number m

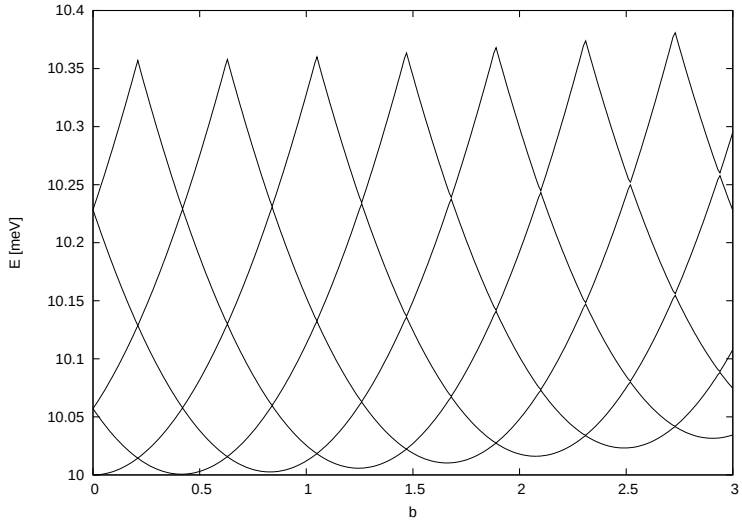

Figure 3.3: Energy spectrum as a function of a magnetic field

It is convenient to separate the Hamiltonian to a B-dependent and a B-independent part $H_{SO} = H_{BSO}(B) + H_{0SO}$ For the B-dependent part (taking the symmetric gauge, $\mathbf{A} = \frac{B}{2}(-y, x, 0)$):

$$\begin{aligned} H_{BSO} &= \frac{\alpha eB}{2\hbar}(-y\sigma_y - x\sigma_x) + \frac{\beta eB}{2\hbar}(-y\sigma_x - x\sigma_y) \\ &= \frac{\alpha eBr}{2\hbar}\begin{pmatrix} 0 & -\cos\theta + i\sin\theta \\ -\cos\theta - i\sin\theta & 0 \end{pmatrix} + \\ &\quad + \frac{\beta eBr}{2\hbar}\begin{pmatrix} 0 & -\sin\theta + i\cos\theta \\ -\sin\theta - i\cos\theta & 0 \end{pmatrix} \\ &= \frac{eBr}{2\hbar}\left(\alpha\begin{pmatrix} 0 & -e^{-i\theta} \\ -e^{i\theta} & 0 \end{pmatrix} + \beta\begin{pmatrix} 0 & -ie^{i\theta} \\ ie^{-i\theta} & 0 \end{pmatrix}\right) \end{aligned}$$

$$\sigma_x = \begin{pmatrix} 0 & 1 \\ 1 & 0 \end{pmatrix}, \sigma_y = \begin{pmatrix} 0 & -i \\ i & 0 \end{pmatrix} \tag{3.12}$$

The matrix elements of this Hamiltonian will be:

$$\langle \varphi_a \mid H_{BSO} \mid \varphi_b \rangle = \frac{Ber}{2\hbar}\int \chi_a(r)\chi_b(r)e^{i(m_b - m_a)\theta}\begin{pmatrix} 0 & -\alpha e^{-i\theta} - i\beta e^{i\theta} \\ -\alpha e^{i\theta} + i\beta e^{-i\theta} & 0 \end{pmatrix} r^2\, dr\, d\theta \tag{3.13}$$

After calculating the angular integral, we get the following five cases:

$$\langle \varphi_a \mid H_{BSO} \mid \varphi_b \rangle = \begin{cases} i\beta I_{HBSO,ab} & \text{for } (m_a - m_b) = 1; \quad a\uparrow, b\downarrow \\ -\alpha I_{HBSO,ab} & \text{for } (m_a - m_b) = -1; \quad a\uparrow, b\downarrow \\ -\alpha I_{HBSO,ab} & \text{for } (m_a - m_b) = 1; \quad a\downarrow, b\uparrow \\ -i\beta I_{HBSO,ab} & \text{for } (m_a - m_b) = -1; \quad a\downarrow, b\uparrow \\ 0 & \text{otherwise} \end{cases} \tag{3.14}$$

Where $I_{HBSO,ab} = \frac{\pi eB}{\hbar}\int \chi_a(r)\chi_b(r)r^2\, dr$.

We need to evaluate also the B-independent Hamiltonian, H_{0SO}:

$$H_{0SO} = \begin{pmatrix} 0 & (\alpha - i\beta)\partial_x + (-i\alpha + \beta)\partial_y \\ (-\alpha - i\beta)\partial_x + (-i\alpha - \beta)\partial_y & 0 \end{pmatrix} \tag{3.15}$$

Using $\partial_x = \cos(\theta)\partial_r - \frac{1}{r}\sin(\theta)\partial_\theta$, $\partial_y = \sin(\theta)\partial_r + \frac{1}{r}\cos(\theta)\partial_\theta$ and rearranging terms, we get

$$H_{0SO} = \begin{pmatrix} 0 & \left(\alpha e^{-i\theta} - i\beta e^{i\theta}\right)\partial_r + \frac{1}{r}\left(-i\alpha e^{-i\theta} + \beta e^{i\theta}\right)\partial_\theta \\ \left(-\alpha e^{i\theta} - i\beta e^{-i\theta}\right)\partial_r + \frac{1}{r}\left(-i\alpha e^{i\theta} - \beta e^{i\theta}\right)\partial_\theta & 0 \end{pmatrix} \tag{3.16}$$

We need the radial and angular partial derivatives of the wavefunctions [1]

$$\begin{aligned}
\frac{\partial}{\partial\rho}(\varphi_{n,m}(\rho,\theta)) &= A_{n,m}e^{-\rho^2/4}\rho^M\left(\left(\frac{2n+M}{\rho}-\frac{\rho}{2}\right)L_n^M(\frac{\rho^2}{2})-\frac{2(n+M)L_{n-1}^M(\frac{\rho^2}{2})}{\rho}\right)\\
&= \varphi_{n,m}(\rho)\left(\frac{M+2n}{\rho}-\frac{\rho}{2}\right)-\frac{A_{n-1,m}}{A_{n,m}}\varphi_{n-1,m}(\rho)\frac{n+M}{\rho}\\
\frac{\partial}{\partial\theta}(\varphi_{n,m}(\rho,\theta)) &= im\varphi_{n,m}(\rho,\theta)
\end{aligned}$$

The matrix elements will look like:

$$\langle\varphi_a \mid H_{0SO} \mid \varphi_b\rangle = 2\pi\lambda\begin{cases} i\beta\,(S_{ab1}-S_{ab2}) & \text{for } (m_a-m_b)=1; \quad a\uparrow, b\downarrow\\ \alpha\,(S_{ab1}+S_{ab2}) & \text{for } (m_a-m_b)=-1; \quad a\uparrow, b\downarrow\\ \alpha\,(S_{ab1}-S_{ab2}) & \text{for } (m_a-m_b)=1; \quad a\downarrow, b\uparrow\\ i\beta\,(-S_{ab1}-S_{ab2}) & \text{for } (m_a-m_b)=-1; \quad a\downarrow, b\uparrow\\ 0 & \text{otherwise}\end{cases} \tag{3.17}$$

Where

$$\begin{aligned}
S_{ab1} &= m_b\int\chi_a(\rho)\chi_b(\rho)\,d\rho\\
S_{ab2} &= \int\chi_a(\rho)\left(\left(M_b-2n_b-\frac{\rho^2}{2}\right)\chi_b(\rho)+2(n_b+M_b)\frac{A_b}{A_{b_-}}\chi_{b_-}(\rho)\right)d\rho
\end{aligned}$$

$b_- = (n_b-1, m_b)$; $\varphi_{-1,m}\equiv 0$ These integrals $S_{ab1,2}$ are also numerically evaluated. Fig 3.4 shows the energy spectrum with the parity of each state identified. It is readily apparent that states with identical parity avoid each other in this B-dependent spectrum, just like it happened in the discrete case.

However, in contrast to the previous section and the Nowak-Szafran paper [13], the gaps do not tend to vanish in the case $\alpha=\beta, g=0$. States are indeed parity-degenerate, but they still display self-avoiding.

3.2.2 Fixed impurity

In this section we will consider a Coulomb impurity located at a small distance z_0 above the plane of the ring. The matrix elements will look like:

$$\langle\varphi_a \mid V_{imp} \mid \varphi_b\rangle = \int\varphi_a^*(r,\theta)\frac{Ke^2}{|\mathbf{r}-\mathbf{r}_0|}\varphi_b(r,\theta)r\,dr\,d\theta \tag{3.18}$$

[1] For the above equation, the derivative of associate Laguerre polynomials was used [20]: $\frac{d}{dx}\left(L_n^\alpha(x)\right) = \frac{nL_n^\alpha(x)-(n+\alpha)L_{n-1}^\alpha(x)}{x}$

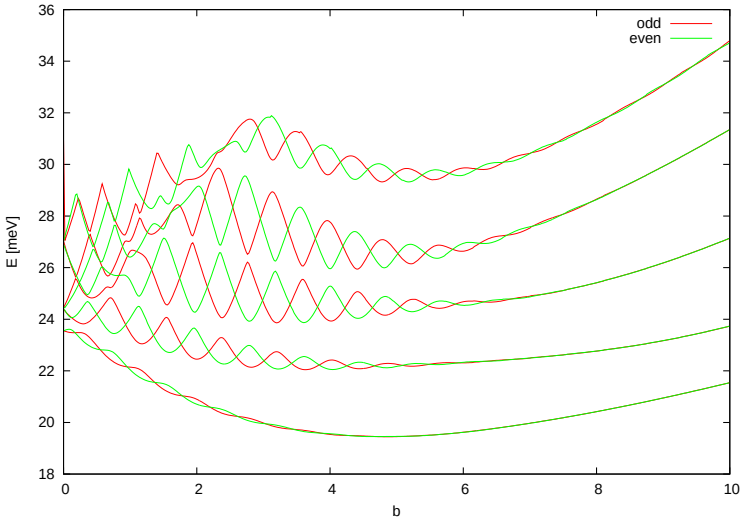

Figure 3.4: Energy spectrum and parity of the first 10 states

This double integral is evaluated numerically. Fig 3.5 shows the charge density in the ring in the case of a negative impurity at coordinates $r = r_0 = 50$nm, $z = 1$nm, $\theta = 0$ with a Coulomb constant $K = 85$ meVnm (this corresponds to $\varepsilon_r = 16.94$). The deformation is quite intuitive, the charge density is nearly zero at the vicinity of the impurity. However, because of the effective periodic potential created by the two kinds of SOI, we see that the maximum density is not centred at the opposite position from the impurity. Fig 3.6 shows the spin orientation around the ring. It seems like it almost mirrors the charge distribution, but there is an inclination caused by SOI and there is a small region around $\theta = \frac{\pi}{2}$ where the spins are flipped. This effect could be of interest since we have an electrostatic field enhancing spin polarization. For smaller magnetic fields we have observed more complicated pictures, for example spin flipping around the impurity. It is probably possible to induce a spin current with a moving probe (similar to an STM) above the ring, but we have not done time-dependent simulations.

3.2.3 Periodic potential

As we have seen that for a 1D ring the SOI is equivalent with a θ-periodic potential, it is interesting to try to find an analogous connection for a 2D ring. We introduce a

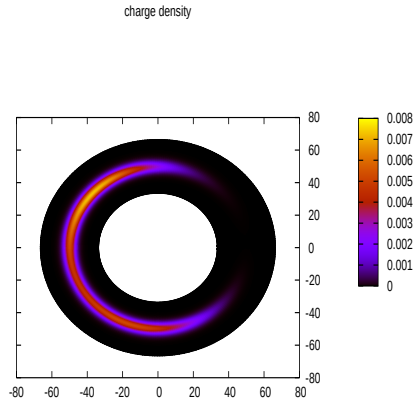

Figure 3.5: Charge density in the presence of a positive impurity

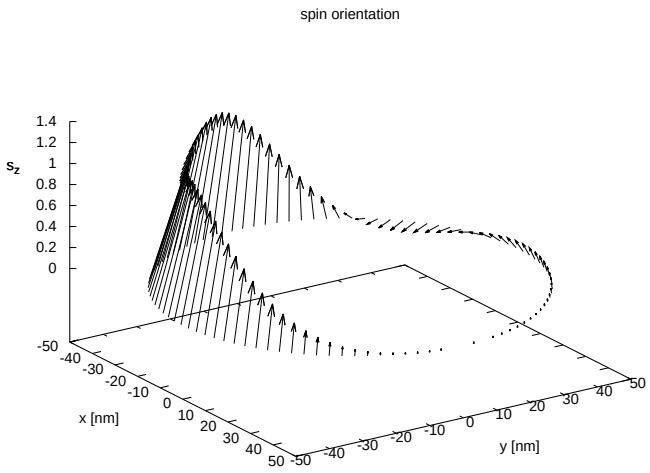

Figure 3.6: Spin density in the presence of a positive impurity

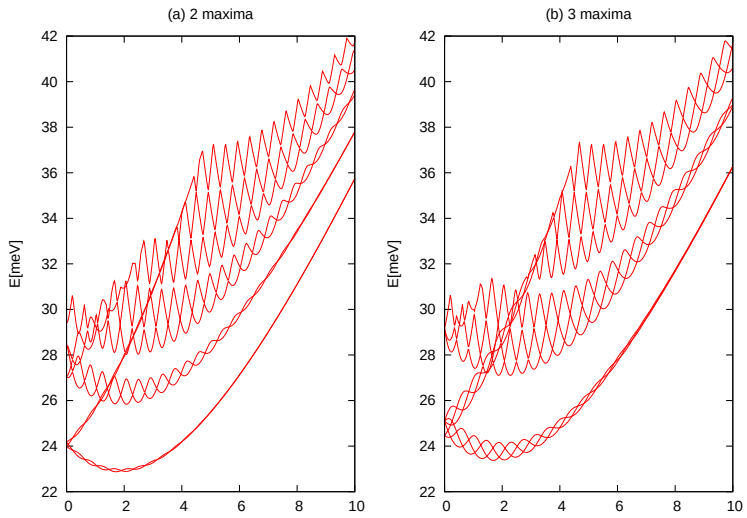

Figure 3.7: Spectra for two (a) and three (b) maxima of the periodic potential as a function of b (x-axis)

periodic potential of the form $V_{per} = V_0 \cos(p\theta), p = 1, 2, 3, \ldots$. The matrix elements will look like:

$$\begin{aligned} \langle \varphi_a \mid V_{per} \mid \varphi_b \rangle &= \int V_0 e^{i(m_b - m_a)\theta} \chi_a(r)\chi_b(r) \frac{1}{2}(e^{ip\theta} + e^{-ip\theta}) r\, dr\, d\theta \\ &= \frac{1}{2} V_0 \int \chi_a(r)\chi_b(r) r\, dr \int \left(e^{i(m_b - m_a + p)\theta} + e^{i(m_b - m_a - p)\theta} \right) d\theta \end{aligned}$$

Because of the angular integral we have:

$$\langle \varphi_a \mid V_{per} \mid \varphi_b \rangle = \begin{cases} \pi V_0 \int \chi_a(r)\chi_b(r) r\, dr & \text{for } (m_a - m_b) = \pm p; \\ 0 & \text{otherwise.} \end{cases} \tag{3.19}$$

It is trivially demonstrable that in the case of a periodic scalar potential, parity will be preserved for an even number of maxima on the ring and destroyed for an odd number. Fig 3.7 shows the spectra. It is apparent that there are certain bands formed by the same number of states as there are maxima in the potential.

3.3 Interacting states

The Coulomb interaction is included, as in the previous chapter, via the exact diagonalization method. The elements U_{abcd} [2] from eq. 2.11 can be calculated:

$$U_{abcd} = \int \varphi_a^*(\mathbf{r})\varphi_b^*(\mathbf{r}')\frac{Ke^2}{|\mathbf{r}-\mathbf{r}'|}\varphi_c(\mathbf{r})\varphi_d(\mathbf{r}')\,dr\,dr'\,d\theta\,d\theta' \tag{3.20}$$

To get rid of the singularity $1/r$, we will use the following expansion in Bessel functions of the first kind [21]:

$$\frac{1}{|\mathbf{r}-\mathbf{r}'|} = \sum_{m=-\infty}^{\infty}\int_0^\infty dk e^{im(\theta-\theta')}J_m(kr)J_m(kr') \tag{3.21}$$

Using this expansion we get

$$\begin{aligned} U_{abcd} &= \sum_{m=-\infty}^{\infty}\int d\theta\,d\theta' e^{i(m_a+m-m_c)\theta}e^{i(m_d+m-m_b)\theta'}\times \\ &\times \int dr\,dr'\chi_a(r)\chi_b(r')\chi_c(r)\chi_d(r')\int dk J_m(kr)J_m(kr')\,dr\,dr' \end{aligned}$$

The angular integrals will be non-zero only if $m = m_c - m_a = m_b - m_d$, so the infinite sum will reduce to a single term. Bearing this in mind:

$$U_{abcd} = 4\pi^2\delta_{(m_c-m_a),(m_b-m_d)}\int dr\,dr'\chi_a(r)\chi_b(r')\chi_c(r)\chi_d(r')\int dk J_m(kr)J_m(kr') \tag{3.22}$$

where $m = m_c - m_a$. If we introduce the following notation:

$$E_{ab}(k) = \int dr\chi_a(r)\chi_b(r)J_{m_a-m_b}(kr) \tag{3.23}$$

Then the integral will look rather simple:

$$U_{abcd} = \int_0^\infty dk E_{ac}(k)E_{bd}(k) \tag{3.24}$$

The biggest advantage of introducing the functions $E_{ab}(k)$ is computational: the values of these functions for various indexes a, b can be stored and a large part of computational redundancy will disappear.

[2] Note that a, b, c, d are indexes of basis states, i.e. not eigenstates.

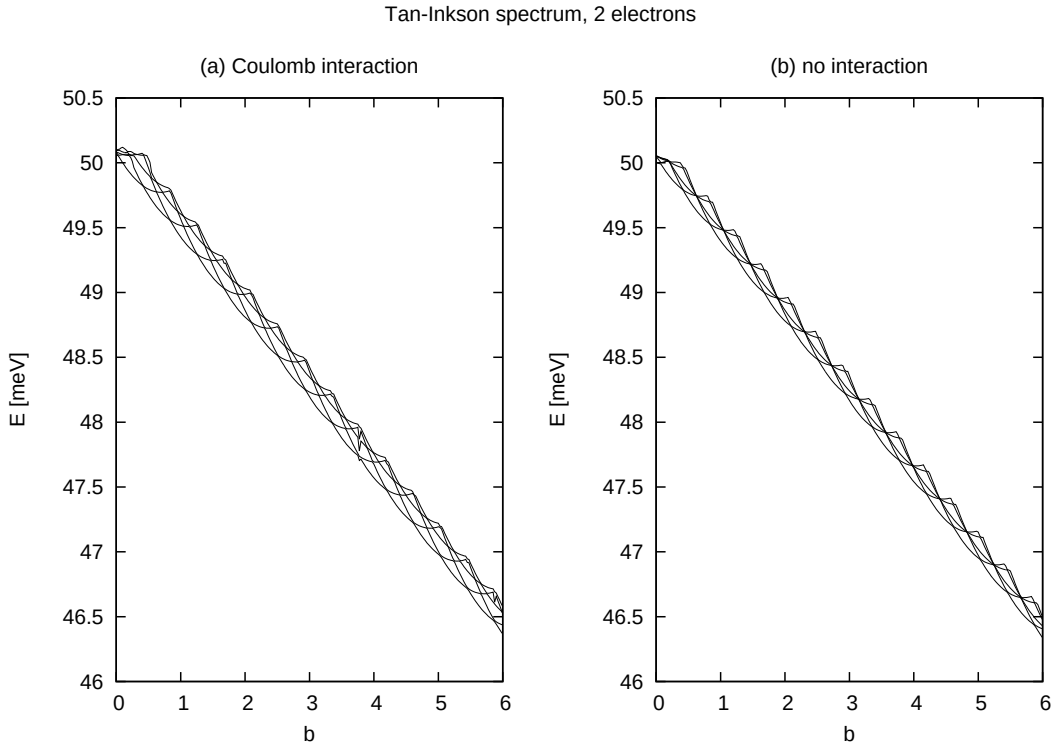

Figure 3.8: Spectra for two electrons with and without Coulomb interaction

It is apparent that there is bigger computational effort in this case than in the case of the discrete model. This was confirmed in practice and I managed to get reliable B-dependent spectra for two interacting electrons, and not more. An example of such spectra is 3.8. The qualitative look of the spectra is similar, but the Coulomb interaction makes energies slightly higher. For this case we used a weaker Coulomb constant of $K = 50$ meVnm for testing, i.e. $\varepsilon_r = 28.8$ and this is why the effect of the interaction does not appear very strong.

Chapter 4

Conclusions

We have modelled a 2D semiconductor ring with radius $r = 100nm$. The primary point of interest was the way the Coulomb interaction changed the effects of spin-orbit coupling.

One of the most important effect discussed in recent times in a ring with both kinds of SOI was charge density deformation with maxima at $\theta = \frac{3\pi}{4}, \frac{7\pi}{4}$. It seems like this effect disappears in the presence of Coulomb repulsion for cases with three or more electrons. However, for the case of exactly two electrons, the effect is actually enhanced. The supposed cause of the charge density deformation is the self-avoiding of states with like parities, but in the case of $N_e = 3, 4$ and Coulomb interaction self-avoiding is still present. This would point to a more complicated relation between the two effects. The analogous effect of spin density deformation, however, is not screened out by the Coulomb effect, on the contrary, its peaks are sharper and with a larger amplitude.

We also examined the way net spin polarization behaves in the presence of SOI and Coulomb repulsion. SOI makes spin transitions more soft, as expected, and at magnetic fields where the Zeeman effect would cause complete polarization, SOI makes polarization fluctuate and less than complete. There are also magnetic fields when SOI makes polarization to be more pronounced than the Zeeman effect would have caused alone. The Coulomb interaction seems to enhance the Zeeman effect, spin polarization happens for smaller magnetic fields than with non-interacting electrons.

Appendix A

Discretization and discrete matrix elements

A.1 1D linear system

Let us take first the simplest possible case, a time-independent Hamiltonian in one dimension. Our sites are at a constant distance a from each other. We will use the effective electron mass m^*.

$$H = -\frac{\hbar^2}{2m^*}\frac{d^2}{dx^2} \tag{A.1}$$

From a Taylor series expansion around $f(x)$ we have the following:

$$f(x+a) = f(x) + af'(x) + \frac{1}{2}a^2 f''(x) + \frac{1}{3!}a^3 f'''x + O(a^4)$$

$$f(x-a) = f(x) - af'(x) + \frac{1}{2}a^2 f''(x) - \frac{1}{3!}a^3 f'''x + O(a^4)$$

hence

$$f''(x) = \frac{f(x+a) + f(x-a) - 2f(x)}{a^2} + O(a^2) \tag{A.2}$$

From A.2 and A.1 we get:

$$Hf(x) = -\frac{\hbar^2}{2m^*}\left[\frac{f(x+a) + f(x-a) - 2f(x)}{a^2}\right] = t\left[2f(x) - f(x+a) - f(x-a)\right] \tag{A.3}$$

Where we introduced the 'hopping parameter' $t = \frac{\hbar^2}{2m^* a^2}$.

As mentioned above, we have a basis in the Hilbert space $\{\mid n\rangle\}$, each basis vector corresponding to a site on the grid. The evaluation of a function on the grid is then $f(x_n) = \langle n \mid f\rangle$. Applying the Hamiltonian to this:

$$\langle n \mid Hf\rangle = t\left[2\langle n \mid f\rangle - \langle n+1 \mid f\rangle - \langle n-1 \mid f\rangle\right] \tag{A.4}$$

$$\sum_m \langle n \mid H \mid m\rangle \langle m \mid f\rangle = t\sum_m \left(2\delta_{nm}\langle m \mid f\rangle - \delta_{n+1,m}\langle m \mid f\rangle - \delta_{n-1,m}\langle m \mid f\rangle\right) \tag{A.5}$$

From where we can identify the matrix elements of the Hamiltonian:

$$\langle n \mid H \mid m\rangle = 2t\delta_{nm} - t\delta_{n+1,m} - t\delta_{n-1,m} = H_{nm} \tag{A.6}$$

The Hamiltonian as an operator looks like this:

$$H = \sum_{nm} \mid n\rangle H_{nm}\langle m \mid = \sum_{nm} \mid n\rangle \left(2t\delta_{nm} - t\delta_{n+1,m} - t\delta_{n-1,m}\right)\langle m \mid \tag{A.7}$$

$$H = \sum_n \left[2t(\mid n\rangle\langle n \mid) - t(\mid n\rangle\langle n+1 \mid) - t(\mid n\rangle\langle n-1 \mid)\right] \tag{A.8}$$

A.2 1D ring system

The Laplacian in polar coordinates r, θ is in general:

$$\nabla^2 = \frac{1}{r}\frac{\partial}{\partial r}\left(r\frac{\partial}{\partial r}\right) + \frac{1}{r^2}\frac{\partial^2}{\partial\theta^2} \tag{A.9}$$

For a constant radius R the Hamiltonian will look like:

$$H_{1D} = -\frac{\hbar^2}{2m^*}\nabla^2 = -\frac{\hbar^2}{2m^*}\frac{1}{R^2}\frac{\partial^2}{\partial\theta^2} \tag{A.10}$$

From A.2

$$\frac{\partial^2}{\partial\theta^2}f(\theta) = \frac{f(\theta+\delta\theta) + f(\theta-\delta\theta) - 2f(\theta)}{\delta\theta^2} \tag{A.11}$$

We will then get the following matrix elements:

$$\langle m \mid H \mid n\rangle = t_\theta\left(2\delta_{mn} - \delta_{m,n+1} - \delta_{m,n-1}\right) \tag{A.12}$$

To implement the periodicity of the system we need to specify:

$$n = N \Rightarrow n + 1 = 1; n = 1 \Rightarrow n - 1 = N \tag{A.13}$$

For example, for $N = 4$ we have:

$$H = t \begin{pmatrix} 2 & -1 & 0 & -1 \\ -1 & 2 & -1 & 0 \\ 0 & -1 & 2 & -1 \\ -1 & 0 & -1 & 2 \end{pmatrix} \tag{A.14}$$

The top right and bottom left elements are the key ones for the periodic nature.

A.2.1 2D ring system

If we have several concentric circles, we need to use the full 2D Laplacian:

$$\nabla^2 = \frac{1}{r}\frac{\partial}{\partial r} + \frac{1}{\partial r^2} + \frac{1}{r^2}\frac{\partial^2}{\partial \theta^2} \tag{A.15}$$

The Hamiltonian looks like:

$$H = -\frac{\hbar^2}{2m^*}\left(\underbrace{\frac{1}{r}\frac{\partial}{\partial r} + \frac{\partial^2}{\partial r^2}}_{H_r} + \underbrace{\frac{1}{r^2}\frac{\partial^2}{\partial \theta^2}}_{H_\theta}\right) = H_r + H_\theta \tag{A.16}$$

We will need the first and second derivatives in r for H_r:

$$f'(r) = \frac{f(r + \delta r) - f(r - \delta r)}{2\delta r} \tag{A.17}$$

$$f''(r) = \frac{f(r + \delta r) + f(r - \delta r) - 2f(r)}{\delta r^2} \tag{A.18}$$

Let k, l be two radial indexes.

$$\langle k \mid H_r \mid l \rangle = t_r \left[\frac{\delta r}{2r}\left(\delta_{k,l-1} - \delta_{k,l+1}\right) + \left(2\delta_{kl} - \delta_{k,l-1} - \delta_{k,l+1}\right)\right] \tag{A.19}$$

Where $t_r = \frac{\hbar^2}{2m^*(\delta r)^2}$. In terms of the natural energy unit $t_R = \frac{\hbar^2}{2m^* R_{ext}^2}$:

$$t_r = t_R \frac{\delta r}{R_e xt}^{\ 2} \tag{A.20}$$

Let us now assume two basis states $|kj\sigma\rangle, |k'j'\sigma'\rangle$, where k, k' are radial indexes, j, j' are angular indexes and σ, σ' are spin indexes. The orbital Hamiltonian will have this matrix element:

$$\begin{aligned}\langle kj\sigma|H_O|k'j'\sigma'\rangle =&\delta_{\sigma\sigma'}\Bigg\{\left[t_\theta + t_r + \frac{t_R}{2}b^2\left(\frac{r_k}{4R_{ext}}\right)^2\right]\delta_{kk'}\delta_{jj'} \\ &-\left[t_\theta + i\frac{bt_B}{4\delta\theta}\right]\delta_{kk'}\delta_{j,j'+1} + t_r\delta_{k,k'+1}\delta_{jj'}\Bigg\} + h.c.\,.\end{aligned} \tag{A.21}$$

Here the orbital effect of the magnetic field is also included, $p = (-i\hbar\nabla + e\mathbf{A})$

A.3 Spin-orbit coupling

We will discuss the calculation of matrix elements of Rashba and Dresselhaus SOI

A.3.1 Rashba SOI

As introduced in 1.2:

$$H_R = \frac{\alpha}{\hbar}\left(\sigma_x p_y - \sigma_y p_x\right) = -i\alpha\left(\sigma_x\partial_y - \sigma_y\partial_x\right) \tag{A.22}$$

And we know that:

$$\partial_x = \cos\theta\partial_r - \frac{1}{r}\sin\theta\partial_\theta \tag{A.23}$$

$$\partial_x = \sin\theta\partial_r + \frac{1}{r}\cos\theta\partial_\theta \tag{A.24}$$

Combining the above, we get:

$$H_R = -i\alpha\left[\frac{1}{r}\left(\sigma_x\cos\theta + \sigma_y\sin\theta\right)\partial_\theta + \left(\sigma_x\sin\theta - \sigma_y\cos\theta\right)\partial_r\right] \tag{A.25}$$

And we can identify the polar spinors σ_r, σ_θ:

$$H_R = -i\alpha\left(\frac{1}{r}\sigma_r\partial_\theta - \sigma_\theta\partial_r\right) \tag{A.26}$$

A.3.2 Dresselhaus SOI

Going through roughly the same steps as in the previous paragraph.

$$H_D = \frac{\beta}{\hbar}\left(\sigma_x p_x - \sigma_y p_y\right) = -i\beta\left(\sigma_x \partial_x - \sigma_y \partial_y\right) \tag{A.27}$$

$$H_D = -i\beta\left[\frac{1}{r}\left(\sigma_x \cos\theta - \sigma_y \sin\theta\right)\partial_\theta - \left(\sigma_x \sin\theta + \sigma_y \cos\theta\right)\partial_r\right] \tag{A.28}$$

It is not difficult to see that in this case the factors in front of the radial operators are complex conjugates[1] of the polar spinors:

$$H_D = -i\beta\left(\frac{1}{r}\sigma_\theta^* \partial_\theta + \sigma_r^* \partial_r\right) \tag{A.29}$$

[1] $\sigma_x^* = \sigma_x$, but $\sigma_y^* = -\sigma_y$

Appendix B

Tan-Inkson eigenstates

The eigenstates of a Tan-Inkson ring can be calculated as follows.

$$V(r) = a_1 r^{-2} + a_2 r^2 - V_0 \tag{B.1}$$

, where $V_0 = \sqrt{a_1 a_2}$. The Tan-Inkson potential has a minimum of $V(r_0) = 0$ at

$$r_0 = \sqrt[4]{\frac{a_1}{a_2}} \tag{B.2}$$

This position defines the radius of the ring. For positions close to the minimum the potential is approximated by a parabolical form:

$$V(r) \approx \frac{1}{2} m^* \omega_0^2 (r - r_0)^2 \tag{B.3}$$

Here m^* is the effective electron mass and the angular frequency is given by

$$\omega_0 = \sqrt{\frac{8a_2}{m^*}} \tag{B.4}$$

The Hamiltonian of the system is:

$$H_0 = \frac{1}{2m^*} P^2 + V \tag{B.5}$$

m^* is the effective electron mass and P is the canonical momentum operator. We consider an external magnetic field normal to the plane of the ring, $\mathbf{B} = B\hat{z}$. The

momentum operator is then given by:

$$P = -i\frac{\hbar}{2m^*}\nabla - e\mathbf{A} \tag{B.6}$$

We will use the vector potential corresponding to the symmetric gauge, namely

$$\mathbf{A} = \left(-\frac{1}{2}By; \frac{1}{2}Bx; 0\right) \tag{B.7}$$

We need to use polar coordinates in two dimensions. The Laplacian is given by:

$$\nabla^2 = \frac{1}{r}\frac{\partial}{\partial r}\left(r\frac{\partial}{\partial r}\right) + \frac{1}{r^2}\frac{\partial^2}{\partial \varphi^2} \tag{B.8}$$

And so the Hamiltonian takes the following form:

$$H_0 = -\frac{\hbar^2}{2m^*}\left(\frac{1}{r}\frac{\partial}{\partial r}\left(r\frac{\partial}{\partial r}\right) + \frac{1}{r^2}\frac{\partial^2}{\partial \varphi^2} + \frac{ieB}{\hbar}\frac{\partial}{\partial \varphi} - \frac{e^2B^2}{4\hbar^2}r^2\right) + \frac{m^*}{8}\omega_0^2 r_0^4\frac{1}{r^2} + \frac{m^*}{8}\omega_0^2 r^2 + \frac{m^*}{4}\omega_0^2 r_0^2 = \tag{B.9}$$

$$= -\frac{\hbar^2}{2m^*}\left(\frac{1}{r}\frac{\partial}{\partial r}\left(r\frac{\partial}{\partial r}\right) + \frac{1}{r^2}\left(\frac{\partial^2}{\partial \varphi^2} - \frac{m^{*2}}{4\hbar^2}\omega_0^2 r_0^4\right) + \frac{ieB}{\hbar}\frac{\partial}{\partial \varphi}\right) + \frac{m^*}{8}\left(\frac{e^2B^2}{m^{*2}} + \omega_0^2\right)r^2 + \frac{m^*}{4}\omega_0^2 r_0^2 = \tag{B.10}$$

$$= -\frac{\hbar^2}{2m^*}\left(\frac{1}{r}\frac{\partial}{\partial r}\left(r\frac{\partial}{\partial r}\right) + \frac{1}{r^2}\left(\frac{\partial^2}{\partial \varphi^2} - \frac{m^{*2}}{4\hbar^2}\omega_0^2 r_0^4\right) + \frac{im^*\omega_c}{\hbar}\frac{\partial}{\partial \varphi}\right) + \frac{1}{8}m^*\omega^2 r^2 + \frac{m^*}{4}\omega_0^2 r_0^2 \tag{B.11}$$

here we introduced the cycloton frequency and the effective cycloton frequencies:

$$\omega_c = \frac{eB}{m^*}$$

$$\omega = \sqrt{\omega_c^2 + \omega_0^2} \tag{B.12}$$

We are looking for the eigenvalues and eigenfunctions of the time-independent Schrödinger equation

$$H_0\Psi = E\Psi \tag{B.13}$$

Because of azimuthal symmetry we can use the factorization

$$\Psi(r,\theta) = u(r)e^{im\theta},\ m = 0,\ \pm1,\ \pm2,\ ... \tag{B.14}$$

which yields the equation:

$$-\frac{\hbar^2}{2m^*}\left(u'' + \frac{1}{r}u' - \left(m^2 + \frac{m^{*2}}{4\hbar^2}\omega_0^2 r^4\right)\frac{1}{r^2}\right) + \frac{1}{8}m^*\omega^2 r^2 u = \left(E - \frac{\hbar\omega_c m}{2} - \frac{m^*}{4}\omega_0^2 r_0^2\right)u \tag{B.15}$$

Which we can rewrite to a simpler form as:

$$-\frac{\hbar^2}{2m^*}\left(u'' + \frac{1}{r}u' - \frac{M^2}{r^2}u\right) + \left(k^2 - \frac{r^2}{4\lambda^4}\right)u = 0 \tag{B.16}$$

with the following notations:

$$M = \sqrt{m^2 + \frac{m^{*^2}}{4\hbar^2}\omega_0^2 r^4} \tag{B.17}$$

$$E - \frac{\hbar\omega_c m}{2} - \frac{m^*}{4}\omega_0^2 r_0^2 = \frac{\hbar^2 k^2}{2m^*} \tag{B.18}$$

and defining the effective magnetic length:

$$\lambda = \sqrt{\frac{\hbar}{m^*\omega}} \tag{B.19}$$

If we scale the radius as $\rho = \frac{r}{\lambda}$ and we use another factorization $u(\rho) = \rho^M \cdot e^{-\frac{1}{4}\rho^2}F(\rho)$ the Schrödinger equation becomes:

$$F'' + \left(\frac{2M+1}{\rho} - \rho\right)F' - \left(M + 1 - k^2\lambda^2\right)F = 0 \tag{B.20}$$

$$s = \frac{1}{2}\rho^2 \tag{B.21}$$

we will get Kummer's equation

$$sF'' + (M + 1 - s)F' - \frac{1}{2}\left(M + 1 - k^2\lambda^2\right)F = 0 \tag{B.22}$$

This equation has two linearly independent solutions:

$$F(s) =_1 F_1(a,\ M+1,\ s) \tag{B.23}$$

and

$$F(s) = s^{-M}\,{}_1F_1(a-M,\,1-M,\,s) \tag{B.24}$$

where $a = \frac{1}{2}\left(M+1-k^2\lambda^2\right)$ and ${}_1F_1(s)$ is the confluent hypergeometric series. In order to have a physically meaningful wavefunction, it must be finite at $s=0$ so the second form B.24 is not satisfactory.

As s grows indefinitely, ${}_1F_1(s)$ diverges like e^s unless:

$$a = -n,\; n = 0,\,1,\,2,\,... \tag{B.25}$$

If the above equation is satisfied, the series becomes a polynomial and the wavefunction can be normalized. Rewriting the equations in terms of n:

$$\frac{1}{2}k^2\lambda^2 = n + \frac{1}{2} + \frac{M}{2} \tag{B.26}$$

$$E = \left(n + \frac{1}{2} + \frac{M}{2}\right)\hbar\omega - \frac{m}{2}\hbar\omega_c - \frac{m^*}{4}\omega_0^2 r_0^2 \tag{B.27}$$

$$\Psi_{n,m}(\rho,\varphi) = C_{n,m}e^{-\frac{1}{4}\rho^2}\rho^M\,{}_1F_1\left(-n,\,M+1,\,\frac{1}{2}\rho^2\right)e^{im\varphi} \tag{B.28}$$

or using the generalized Laguerre's polynomials:

$$\Psi_{n,m}(\rho,\varphi) = \frac{C_{n,m}\Gamma(M+1)n!}{\Gamma(M+n+1)}e^{-\frac{1}{4}\rho^2}\rho^M L_n^M\left(\frac{1}{2}\rho^2\right)e^{im\varphi} \tag{B.29}$$

if we use the normalization relation of the generalized Laguerre's polynomials [20]:

$$\int_0^\infty e^{-x}x^\alpha L_n^\alpha(x)L_m^\alpha(x)dx = \frac{\Gamma(\alpha+n+1)}{n!}\delta_{mn} \tag{B.30}$$

and require the wavefunction to be normalized:

$$2\pi\int_0^\infty |\Psi_{n,m}|^2\,r dr = 1 \tag{B.31}$$

We get the normalization factors

$$C_{n,m} = \frac{1}{\lambda^{M+1}}\sqrt{\frac{\Gamma(M+n+1)}{2^{M+1}\left(\Gamma(M+1)\right)^2 n!\pi}} \tag{B.32}$$

Bibliography

[1] J. Fabian, A. Matos-Abiaguea, C. Ertlera, P. Stano, and I. Zutic, *Semiconductor spintronics*. Slovak Academy of Sciences, Bratislava, 2002.

[2] E. I. Rashba, "Spin-orbit coupling and spin transport," *arXiv cond-mat*, vol. 0507007v2:5, 2005.

[3] S. Bandyopadhyay and M. Cahay, *Introduction to Spintronics*. CRC Press, Boca Raton, 2008.

[4] S. Datta and B. Das, "Electronic analog of the electro-optic modulator," *Appl. Phys. Lett*, vol. 56, no. 7, pp. 665–667, 1990.

[5] J. Wunderlich, B.-G. Park, A. C. Irvine, L. P. Zârbo, E. Rozkotová, P. Nemec, V. Novák, J. Sinova, and T. Jungwirth, "Spin hall effect transistor," *Science*, vol. 330, pp. 1801–1804, 2010.

[6] M. Johnson and R. Silsbee, "Interfacial charge-spin coupling: Injection and detection of spin magnetization in metals," *Phys. Rev. Lett.*, vol. 55, p. 1790, 1985.

[7] Y. A. Bychkov and E. I. Rashba, "Oscillatory effects and the magnetic susceptibility of carriers in inversion layers," *J. Phys. C*, vol. 74, p. 6039, 1984.

[8] G. Dresselhaus, "Spin-orbit coupling effects in zinc blende structures," *Phys. Rev.*, vol. 98, p. 368, 1955.

[9] R. Winkler, *Spin orbit coupling effects in two-dimensional electron and hole systems*. Springer-Verlag Berlin, Heidelberg, New York, 2003.

[10] E. Zipper, M. Kupas, J. Sadowski, and M. M. Maska, "Spin relaxation in semiconductor quantum rings and dots - a comparative study," *JPCM*, vol. 23, p. 115302, 2011.

[11] Y. Liu, F. Cheng, X. J. Li, F. M. Peeters, and K. Chang, "Tuning of the two electron states in quantum rings through the spin-orbit interaction," *Phys. Rev. B*, vol. 82, p. 045312, 2010.

[12] B. Molnár, F. M. Peeters, and P. Vasilopoulos, "Spin-dependent magnetotransport through a ring due to spin-orbit interaction," *Phys. Rev. B*, vol. 69, p. 155335, 2004.

[13] M. P. Nowak and B. Szafran, "Spin-orbit coupling effects in two-dimensional circular quantum rings: Elliptical deformation of confined electron density," *Phys. Rev. B*, vol. 80, p. 195319, 2009.

[14] J. S. Sheng and K. Chang, "Spin states and persistent currents in mesoscopic rings: Spin-orbit interactions," *Phys. Rev. B*, vol. 74, pp. 235315:1–14, 2006.

[15] J. Schliemann, J. C. Egues, and D. Loss, "Nonballistic spin-field-effect transistor," *Phys. Rev. Letters*, vol. 90, pp. 146801:1–4, 2003.

[16] J. Splettstoesser, M. Governale, and U. Zülicke, "Persistent current in ballistic mesoscopic rings with rashba spin-orbit coupling," *Phys. Rev. B*, vol. 68, p. 165341, 2003.

[17] F. E. Meijer, A. F. Morpurgo, and T. M. Klapwijk, "One-dimensional ring in the presence of rashba spin-orbit interaction: Derivation of the correct hamiltonian," *Phys. Rev. B*, vol. 66, p. 033107, 2002.

[18] A. L. Fetter and J. D. Walecka, *Quantum Theory of Many-Particle Systems*. Dover Publications, 2003.

[19] W.-C. Tan and J. Inkson, "Electron states in a two-dimensional ring - an exactly soluble model," *Semicond. Sci. Technol.*, vol. 11, 1996.

[20] I. S. Gradshteyn and I. Ryzhik, *Table of integrals, series, and products*. Academic Press, 2007.

[21] J. D. Jackson, *Classical electrodynamics*. John Wiley and Sons, 1999.